Journal of Solid State Chemistry 184 (2011) 1566–1570

Contents lists available at ScienceDirect

Journal of Solid State Chemistry

journal homepage: www.elsevier.com/locate/jssc

A re-investigation of the crystal structure and luminescence of $BaCa_2MgSi_2O_8:Eu^{2+}$

Cheol-Hee Park [a,*], Tae-Hoon Kim [a], Yoshinori Yonesaki [b], Nobuhiro Kumada [b]

[a] LG Chem Research Park, Daejeon 305-380, Republic of Korea
[b] University of Yamanashi, Miyamae-Cho 7-32, Kofu 400-8511, Japan

ARTICLE INFO

Article history:
Received 4 March 2011
Received in revised form
13 April 2011
Accepted 17 April 2011
Available online 22 April 2011

Keywords:
Barium calcium magnesium silicate
$BaCa_2MgSi_2O_8$
Crystal structure
Neutron diffraction data
Eu^{2+} luminescence
Site assignment

ABSTRACT

Barium calcium magnesium silicate ($BaCa_2MgSi_2O_8$), a compound whose space group was obtained via X-ray diffraction data, was re-investigated using neutron diffraction techniques. A combined powder X-ray and neutron Rietveld method revealed that $BaCa_2MgSi_2O_8$ crystallizes in the trigonal space group $P\bar{3}$ ($Z=1$, $a=5.42708(5)$ Å, $c=6.79455(7)$ Å, $V=173.310(4)$ Å^3; $R_p/R_{wp}=5.52\%/7.63\%$), instead of the previously believed space group $P\bar{3}m1$. The difference in the two structures arises from the displacement of the O2 atom. Blue emission from $Ba_{0.98}Eu_{0.02}Ca_2MgSi_2O_8$ under 325-nm excitation is ascribed to the $4f^65d^1 \rightarrow 4f^7$ transitions of Eu^{2+} ions at Ba sites and Ca sites. Site assignment of Eu^{2+} ions in the titled compound was performed by analysis of emission spectra at temperatures in the range of 4.2–300 K.

1. Introduction

Phosphors activated with Eu^{2+} are widely used in implements that individuals use in daily life such as lamps in copying machine with $(Sr,Mg)_2P_2O_7:Eu^{2+}$, a blue component of three-band fluorescent lamps and plasma display panels (PDPs) with $BaMgAl_{10}O_{17}:Eu^{2+}$, and a storage phosphor for X-ray imaging with $Ba(F,Br):Eu^{2+}$ [1]. The luminescence of the Eu^{2+} ion in inorganic hosts is generally associated with transitions between the $^8S_{7/2}$ ($4f^7$) ground state and the crystal field components of the $4f^65d^1$ excited-state configurations. The energetic position of the emission band is strongly dependent on the host crystal, changing from near UV to red. Silicates of $M_3MgSi_2O_8$ (M=Ba, Sr, and Ca) have received recent attention because Eu^{2+}- and/or Mn^{2+}-doped powders have exhibited efficacy in white-light devices and PDPs [2–9]. The luminescence of $M_3MgSi_2O_8:Eu^{2+}$ is highly efficient and its color is tunable by changing molar ratios of Ba, Sr and Ca. High durability against vacuum ultraviolet radiation is also reported in $(Ba, Sr)_3MgSi_2O_8:Eu^{2+}$ [5].

The luminescence properties of Eu^{2+} are highly sensitive to its local environment, making it essential to establish the correct crystal structures of $M_3MgSi_2O_8$. Since the report by Klasens and co-workers[10], all the compounds of $M_3MgSi_2O_8$ have been assumed to be isostructural to the mineral merwinite, $Ca_3MgSi_2O_8$, which was initially assigned an orthorhombic structure [10]. At a later date, Moore and Araki [11] revised the structure to a monoclinic type. Aitasalo et al. [12] found that the compound with M=Ba is not isostructural to the merwinite, but crystallizes in a trigonal structure. In the following years, Yonesaki et al. [8,9] investigated crystal structures of $M_3MgSi_2O_8$ using X-ray diffraction techniques and reported that $Ba_3MgSi_2O_8$ has the $K_3NaS_2O_8$-type trigonal structure with the space group $P\bar{3}m1$. However, the $\sqrt{3}\times\sqrt{3}\times 1$ superstructure of $Ba_3MgSi_2O_8$ with the space group $P\bar{3}$ could not be observed from X-ray diffraction data [12,13] and was not identified until Park and co-workers conducted a neutron diffraction study [13].

The structure of another member $M_3=BaCa_2$ was also reported to have the $K_3NaS_2O_8$-type structure, and luminescent properties of Eu^{2+} in the compound were explained based on its crystal structure [8]. However, the average Si–O distance in the reported structure, 1.586 Å, is shorter than the expected value of the sum of ionic radii: d(Si–O)=1.64 Å [8,14]. This discrepancy suggests that the $BaCa_2MgSi_2O_8$ structure may be incorrect. Based on this study, we have re-investigated the crystal structure of $BaCa_2MgSi_2O_8$ and the luminescent properties of Eu^{2+} in the compound using neutron powder diffraction and low-temperature photoluminescence techniques.

2. Experimental

The starting materials were $BaCO_3$ (99.95%, Alfa), $CaCO_3$ (99.99%, High Purity Chemicals), MgO (99.99%, High Purity Chemicals),

* Corresponding author. Fax: +82 42 861 2057.
E-mail address: pmoka@lgchem.com (C.-H. Park).

0022-4596/$ - see front matter © 2011 Elsevier Inc. All rights reserved.
doi:10.1016/j.jssc.2011.04.030

Eu_2O_3 (99.95%, Kanto Chemical Co., Inc.) and SiO_2 (99.99%, 1–3 mm pieces, Cerac). Prior to use, pieces of SiO_2 were ground into a fine powder with an alumina mortar and pestle. Polycrystalline $BaCa_2MgSi_2O_8$ was prepared by heating the stoichiometric mixture at 1423 K for 15 h in air followed by cooling and grinding and then reheating at 1423 K for 15 h in air. The powder of $Ba_{0.98}Eu_{0.02}Ca_2MgSi_2O_8$ was prepared by heating the stoichiometric mixture of the starting reagents at 1373 K for 4 h in a flow of 2% $H_2(g)-98\%$ $N_2(g)$.

The powder X-ray diffraction (XRD) data was collected at room temperature on a Bragg–Brentano diffractometer (Bruker-AXS Advance D8) with a Cu X-ray tube, a focusing primary Ge (1 1 1) monochromator ($\lambda=1.5406$ Å), and a position sensitive Väntec detector over an angular range of $10^\circ \le 2\theta \le 151^\circ$ with a step of 0.016671° and a total measurement time duration of 45 h.

The neutron powder diffraction data was collected at room temperature in air using the HRPD installed at the research reactor HANARO (30 MW) in the Korea Atomic Energy Research Institute (KAERI). The HANARO HRPD system is equipped with a combination of collimators, $C_1/C_2/C_3=20'/30'/10'$ and a vertically focusing mosaic monochromator (Ge (3 3 1) crystals, $\lambda=1.8349$ Å). The data was collected over the 2θ range of $10-160^\circ$ with a step of 0.05° and a total measurement time of 3 h.

Structure determination and refinement were performed using TOPAS software [15].

Photoluminescence measurements were made with the 325-nm line of a He–Cd continuous-wave laser (Omnichrome 2074) for excitation and a charge-coupled detector (Hamamatsu, C7042) for detection. Variable-temperature spectra were recorded by a cryostat (Letbold, REF-1052M-4k5W) in the temperature range of 4.2–300 K.

3. Results and discussion

3.1. Powder X-ray and neutron diffraction analysis

The X-ray diffraction pattern of $BaCa_2MgSi_2O_8$ was well indexed with a hexagonal unit cell with $a_0=5.427$ and $c_0=6.795$ Å. Previously, Yonesaki and co-workers determined via powder X-ray diffraction that $BaCa_2MgSi_2O_8$ has the $K_3NaS_2O_8$ ($P\bar{3}m1$)-type structure [8]. Adoption of their reported structure resulted in a good Rietveld profile fitting with $R_p/R_{wp}=6.18\%/8.55\%$. However, the atomic displacement parameter (ADP) for atom O2 was unusually large, and the average Si–O distance of 1.56 Å was much shorter than the expected value calculated from the sum of ionic radii: d (Si–O)=1.64 Å [14]. The bond valence sums [16] were calculated using the software Valence [17] for the $BaCa_2MgSi_2O_8$ crystal structure ($P\bar{3}m1$) obtained from the X-ray diffraction data. The sums were: 2.11 (Ba), 1.65 (Ca), 1.94 (Mg), 5.05 (Si), 1.98 (O1), and 2.25 v.u. (O2). The bond valence model has been widely used to check and validate newly determined structures [18]. The abnormally high valence sum of 5.05 for Si suggests that the structural model was an approximation.

The O2 site ($6i$) is constrained to (x, $\bar{x}$, z) in the space group $P\bar{3}m1$, while it is a general position (x, y, z) in an equivalent structural model for the space group $P\bar{3}$, a subgroup of $P\bar{3}m1$. Symmetry reduction to $P\bar{3}$, therefore, allows for independent refinements of positional parameters of x and y. Rietveld refinement of the X-ray diffraction data led to an average Si–O distance of 1.59 Å and a reduced ADP for atom O2 (from 2.6 to 0.3 $Å^2$ of B_{iso}) with R_p of 5.72%. The refined atom parameters from the X-ray diffraction data for the two space groups ($P\bar{3}$ and $P\bar{3}m1$) are provided in the Supporting Information. Comparison of refinement results from the X-ray diffraction data for the two space groups, however, did not clearly show the correct space group for $BaCa_2MgSi_2O_8$.

In order to confirm the crystal structure, neutron diffraction data was collected. This data is essential for the determination and confirmation of the structure, especially when used in conjunction with X-ray data. The O atom has the smallest X-ray atomic scattering, while the neutron scattering length for the O atom ($b_{c,O}=5.803$) is higher than those for Si ($b_{c,Si}=4.149$), Mg ($b_{c,Mg}=5.375$), Ca ($b_{c,Ca}=4.70$), and the much heavier Ba ($b_{c,Ba}=5.07$). The Bragg peaks in the neutron diffraction data were completely indexed with the $P\bar{3}m1$ unit cell, excluding the possibility of a superstructure. An acceptable fit of the neutron diffraction data, however, could not be obtained with the $P\bar{3}m1$ space group. Following symmetry reduction to $P\bar{3}$, convergence was achieved with reasonable Si–O distances, ADPs, and reduced residuals (from 17.1 to 5.1% of R_p), indicating that $P\bar{3}$ is the correct space group for $BaCa_2MgSi_2O_8$.

A combined Rietveld refinement of the X-ray and neutron diffraction data was employed to complete the structural determination. The refinement parameters included: scale factors, background, unit-cell parameters, peak-profile coefficients, atomic coordinates, and isotropic thermal parameters. The residual factors were $R_p/R_{wp}=5.91\%/8.19\%$ for X-ray data, 5.22%/7.17% for neutron data, and 5.52%/7.63% for the combined data. The final profile fits are shown in Fig. 1, and powder

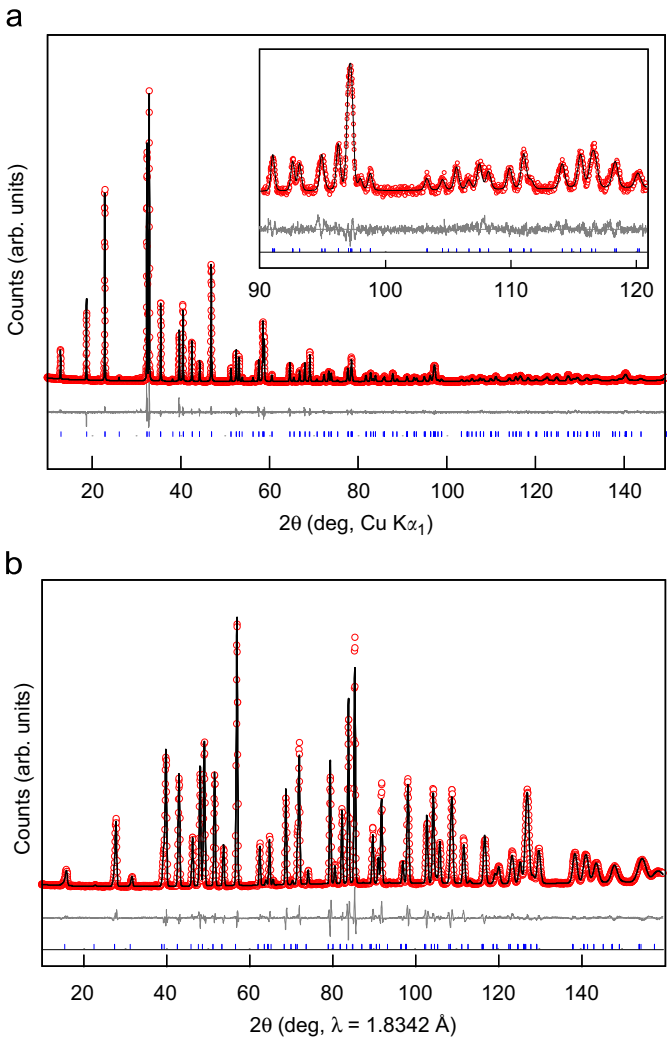

Fig. 1. Combined (a) X-ray ($\lambda=1.5406$ Å) and (b) neutron ($\lambda=1.8342$ Å) Rietveld refinement profiles for $BaCa_2MgSi_2O_8$ recorded at room temperature. The circle line marks experimental points and the solid line is the calculated profile. The lower trace shows the difference curve, and the ticks denote expected peak positions for $BaCa_2MgSi_2O_8$. The inset shows the high-angle data in detail.

Table 1
Results of structure refinement for $BaCa_2MgSi_2O_8$ from combined powder X-ray and neutron diffraction data.

Chemical formula	$BaCa_2MgSi_2O_8$
Formula weight	425.951
Space group	$P\bar{3}$ (No. 147)
Z	1
a (Å)	5.42708(5)
c (Å)	6.79455(7)
V (Å^3)	173.310(4)
d_{calc} (g/cm^3)	4.08119(9)
Temperature (K)	296
Number of reflections (X-ray/neutron)	242/158
$R_p/R_{wp}/R_{exp}/R_B$ (X-ray) (%)[a]	5.91/8.19/3.63/3.29
$R_p/R_{wp}/R_{exp}/R_B$ (neutron) (%)[a]	5.22/7.17/1.89/1.95
R_p/R_{wp} (total) (%)[a]	5.52/7.63
Goodness of fit (%, total)	2.74
Total refined parameters (P)	31

[a] $R_p=\Sigma|Y_{o,m}-Y_{c,m}|/\Sigma|Y_{o,m}|$; $R_{wp}=(\Sigma w_m|Y_{o,m}-Y_{c,m}|^2/\Sigma w_m|Y_{o,m}|^2)^{1/2}$; $R_B=(\Sigma|I_{o,k}-I_{c,k}|/\Sigma I_{o,k})$; $R_{exp}=(|M-P|/\Sigma w_m|Y_{o,m}|^2)^{1/2}$; $\chi^2=(R_{wp}/R_{exp})^2$; and $w_m=1/Y_{o,m}$.

Table 2
Atomic coordinates and isotropic displacement (Å$^2\times10^2$) for $BaCa_2MgSi_2O_8$ at room temperature.

Atom	Site	x	y	z	B_{iso} (Å^2)
Ba1	1*b*	0	0	0.5	0.28(4)
Ca1	2*d*	1/3	2/3	0.8402(2)	0.66(2)
Mg1	1*a*	0	0	0	0.35(2)
Si	2*d*	1/3	2/3	0.2739(2)	0.20(3)
O1	2*d*	1/3	2/3	0.5096(2)	0.70(3)
O2	6*g*	0.12215(16)	−0.23168(14)	0.17652(14)	0.70(2)

Table 3
Interatomic distances (Å) and selected angles (deg) in $BaCa_2MgSi_2O_8$ at room temperature.

Ba–O1 × 6	3.13400(5)	O1–Ba–O1	60.043(3)
Ba–O2 × 6	2.7721(10)	O1–Ba–O2	77.08(3)
Ca–O1	2.246(2)	O2–Ba–O2	63.71(3)
Ca–O2 × 3	2.4209(6)	O1–Ca–O2	87.31(4)
Ca–O2 × 3	2.7336(15)	O2–Ca–O2	119.782(9)
Mg1–O2 × 6	2.0718(10)	O2–Ca–O2′	69.08(4)
Si1–O1	1.602(2)	O2′–Ca–O2′	56.75(4)
Si1–O2 × 3	1.6395(12)	O2–Mg–O2	89.85(4)
		O1–Si–O2	113.80(6)
		O2–Si–O2	104.81(7)

refinement results are given in Table 1. The refined atomic and isotropic displacement parameters can be seen in Table 2, and the important bond distances and angles are listed in Table 3.

The bond valence sums for the structure ($P\bar{3}$) determined from the combined data are: 2.21 (Ba), 1.73 (Ca), 2.15 (Mg), 4.11 (Si), 1.88 (O1), and 2.05 v.u. (O2). These values closely match the expected charges of the ions.

3.2. The crystal structure

The crystal structure of $BaCa_2MgSi_2O_8$ is depicted in Fig. 2, where SiO_4 tetrahedra and MgO_6 octahedra build polyhedral networks along the *ab* plane. The SiO_4 tetrahedron shares corners with three MgO_6 octahedra and an apex with Ca and Ba atoms, while the MgO_6 octahedra are linked at every corner by six SiO_4 tetrahedra. The basic structural building units in $BaCa_2MgSi_2O_8$

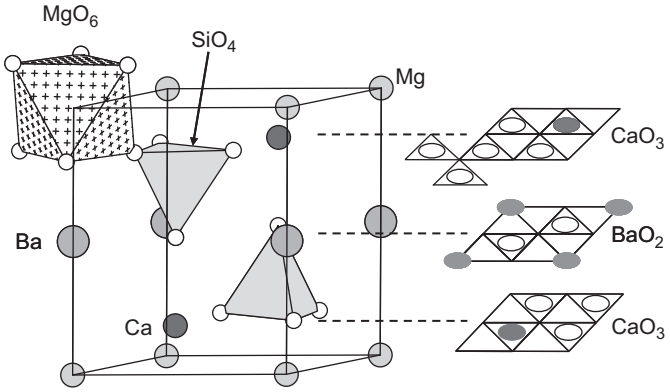

Fig. 2. Crystal structure of $BaCa_2MgSi_2O_8$.

are similar to those in $Ba_3MgSi_2O_8$ and $Ca_3MgSi_2O_8$ [8,13]. The structure may also be described as a stacking of one [BaO_2] and two [CaO_3] layers, like the 3-layer stacking of one [BaO_2] and two [BaO_3] layers in $Ba_3MgSi_2O_8$ [13]. The Mg atoms occupy distorted octahedral sites formed by two adjacent [CaO_3] layers, while the Si atoms occupy tetrahedral sites formed by the [BaO_2] layer and the [CaO_3] layer. The Ba atom binds six O2 atoms and six O1 atoms; the O2 atoms form a distorted octahedron environment with Ba–O2 distance of 2.7721(10) Å and the O1 atoms are in a distorted hexagonal plane in the equatorial position of the Ba atom with Ba–O1 distance of 3.1340(5) Å. The site symmetry is S_6 ($\bar{3}$) (Fig. 3a). The Ca atom resides at the seven-coordinated site. Three O2 atoms are in a trigonal plane below the Ca atom with Ca–O2 distance of 2.7336(15) Å and three O2 atoms are in a trigonal plane slightly above the Ca atom with Ca–O2 distance of 2.4209(6) Å. One O1 atom is in a capping position with Ca-O1 distance of 2.246(2) Å. The symmetry for the Ca site is C_3 (3) (Fig. 3b).

The structure of $BaCa_2MgSi_2O_8$ ($P\bar{3}$) is compared with the X-ray diffraction structure ($P\bar{3}m1$) in Fig. 4. Projection onto the *ab* plane reveals the difference between the two structures. In the $P\bar{3}m1$ structure projected on the *ab* plane, O2 atoms lie on the straight lines joining atoms Mg and Si, while O2 atoms in the $P\bar{3}$ structure lie off these lines, resulting in re-orientations of MgO_6 octahedra and SiO_4 tetrahedra. In the refined structures, the bond angles Mg–O2–Si are 170.77(10)° for the $P\bar{3}m1$ structure and 158.4(3)° for the $P\bar{3}$ structure. Rotation of the polyhedra and the loss of mirror symmetry in the $P\bar{3}$ structure arise from the displacement of the O2 atom relative to its position in the $P\bar{3}m1$ structure. The refined O2 positions are (0.1222, −0.2317, and 0.1765) for the $P\bar{3}$ structure (Table 2) and (0.1843, −0.1843, and 0.1770) for the $P\bar{3}m1$ structure (Supporting Information). The shift in the position between the two structures is calculated to be 0.31 Å.

3.3. Luminescence

$Ba_{0.98}Eu_{0.02}Ca_2MgSi_2O_8$ exhibits an intense blue emission under ultraviolet excitation, which supports previous research [8]. The emission spectrum of the compound ($\lambda_{exc}=325$ nm) measured at 4.2 K reveals a broad band around 430 nm with a shoulder on the long-wavelength side (Fig. 5). The emission spectrum can be fit to two Gaussian profiles; one centered at 430 nm (23,300 cm^{-1}) and the second centered at 460 nm (21,700 cm^{-1}). The two profiles correspond to the $4f^65d^1\rightarrow4f^7$ transitions of Eu^{2+} ions at Ba sites and Ca sites in $BaCa_2MgSi_2O_8$. Yonesaki and co workers observed the emission of $Ba_{0.98}Eu_{0.02}Ca_2MgSi_2O_8$ at room temperature under 254-nm excitation, and fit the spectrum with two Gaussian peaks at 430 and 450 nm. They assigned the emission at 430 nm to Eu^{2+} in the Ca site, and

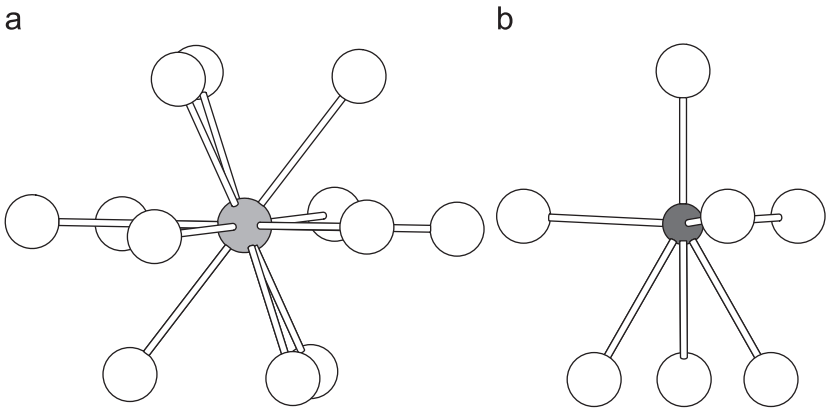

Fig. 3. Coordination environments about (a) the Ba atom and (b) the Ca atom in $BaCa_2MgSi_2O_8$. The filled circles represent the Ba atom and the Ca atom, and the larger open circles represent O atoms.

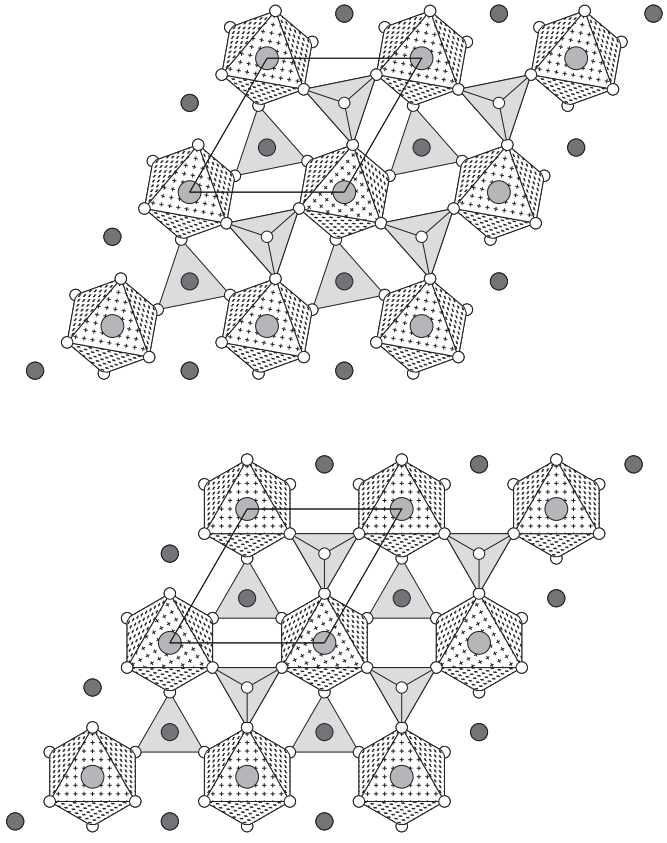

Fig. 4. The $P\bar{3}$ structure (top) and the $P\bar{3}m1$ structure (bottom) projected onto the *ab* plane.

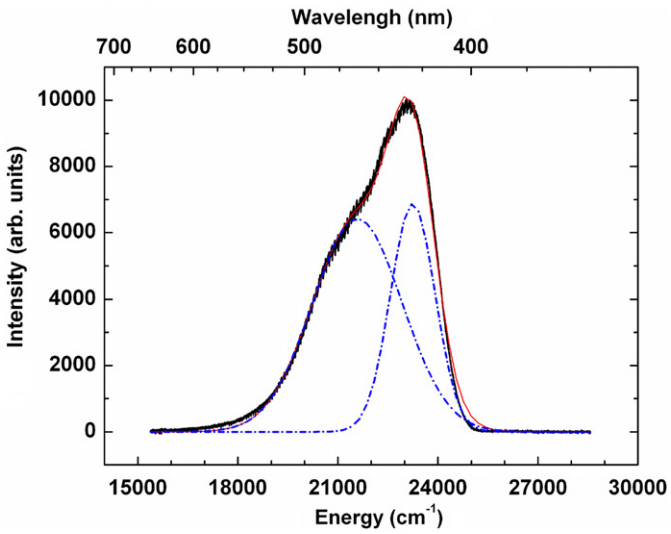

Fig. 5. Emission spectrum of $Ba_{0.98}Eu_{0.02}Ca_2MgSi_2O_8$ obtained at 4.2 K under excitation at 325 nm. Dash-dotted lines are best-fit Gaussian profiles.

the other to the Ba site using Van Uitert's empirical equation [19]. For the calculation they assumed that the Ba site is only six-coordinated, not twelve-coordinated, because the six Ba–O2 distances are much shorter (2.82 Å) than the six Ba–O1 distances (3.01 Å). However, a Ba–O distance close to 3 Å is observed in a number of oxides [8,13,20]. The equation with the twelve coordination of the Ba site suggests the emission at 430 nm corresponds to the Ba site, not the Ca site. This is supported by the observation that Eu^{2+} emission in Ca sites occurs at longer wavelengths than in Ba sites in many luminescent materials [21]. It can be rationalized using the crystal field theory. The emission occurs from the lowest crystal field component of the $4f^65d^1$ configuration to the ground state level (^8S from $4f^7$) of Eu^{2+}. At the smaller atom site, Eu^{2+} ion experiences a higher crystal field than it would at a larger atom site, which pushes the lowest crystal field component of the $4f^65d^1$ configuration to a lower energy. Since the electrons of the 4*f* orbital are screened by the filled 5*s* and 5*d* orbitals, the energy of the ground state level is minimally affected by the crystal field. In conclusion, the emission is observed at a longer wavelength. A simplified energy level scheme of the Eu^{2+} ion with different crystal field strength is depicted in Fig. 6. The integrated intensities of the two emission bands also suggest that the emission at the longer wavelength corresponds to the Ca site. The area of the Gaussian at 460 nm is 1.9 times larger than the one at 430 nm. Considering that the multiplicity of the Ca site is twice than that of the Ba site, the emission at 460 nm is ascribed to Eu^{2+} in the Ca site, and the one at 430 nm is from Eu^{2+} in the Ba site.

By increasing the temperature from 4.2 to 300 K, the maximum intensities of both emission bands decreased by about 30%, and their full width at half-maximum (FWHM) increased by about 20% (Fig. 7), which is related to the increase in thermal occupancy in high-order vibrational states [22]. No additional emission band was observed over the range 350–650 nm with increasing temperature. When the temperature is increased from 4.2 to 300 K, the integrated emission intensity drops by 22% for the emission at 430 nm and by 28% for the emission at 450 nm. It is worth noting that in isomorphous host lattices, Eu^{2+} emission in Ca site exhibits stronger thermal quenching behavior than in Ba

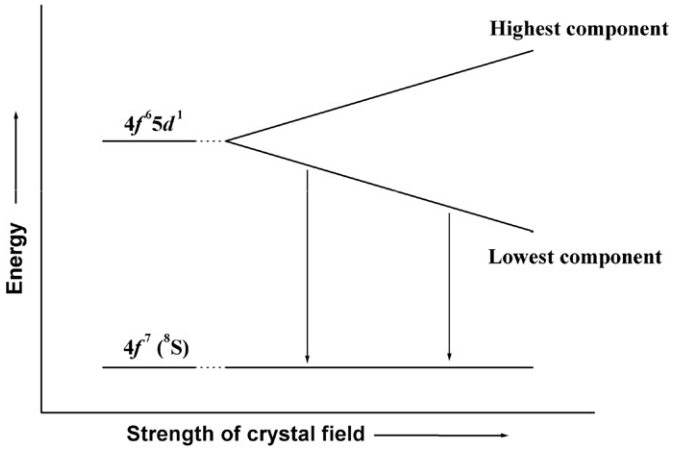

Fig. 6. A simplified energy level scheme of the Eu^{2+} ion with different crystal field strength.

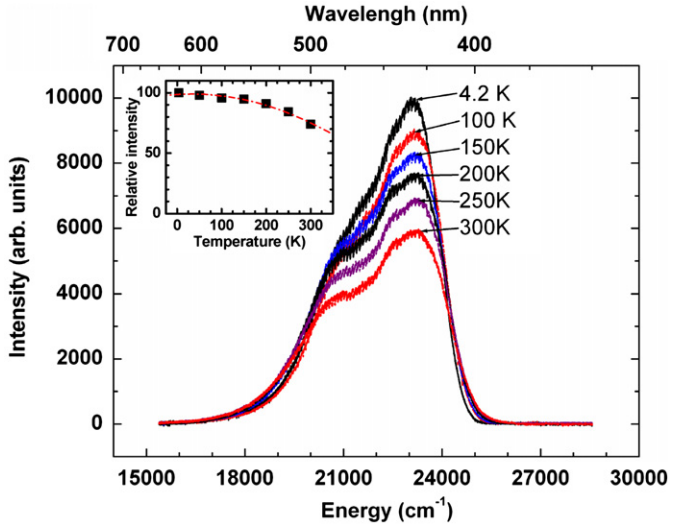

Fig. 7. Emission spectra of $Ba_{0.98}Eu_{0.02}Ca_2MgSi_2O_8$ measured at different temperatures from 4.2 to 300 K under excitation at 325 nm. The inset shows the integrated intensity of the emission as a function of the temperature.

site [23]. For example, the temperatures where the light output decreased to 50% of the value at 77 K is 505 K for M=Ca and 545 K for M=Ba in $M_3MgSi_2O_8$:Eu^{2+}, and 390 K for M=Ca and 420 K for M=Ba in M_2SiO_4:Eu^{2+} [24].

4. Conclusions

The compound of $BaCa_2MgSi_2O_8$ has been re-investigated using a neutron diffraction technique. A combined powder X-ray and neutron Rietveld method reveals that $BaCa_2MgSi_2O_8$ crystallizes in the space group $P\bar{3}$, instead of the space group $P\bar{3}m1$, which was previously determined from only X-ray diffraction data. The difference in the two structures arises from the displacement of the O2 atom relative to its position in the $P\bar{3}m1$ structure. Careful analysis of the X-ray diffraction data favors the $P\bar{3}$ structure, however, both structures obtained from only X-ray diffraction data are unsatisfactory. In order to identify Eu^{2+} sites in the titled compound, emission spectra were measured at various temperatures in the range of 4.2–300 K. The site assignments of Eu^{2+} ions using Van Uitert's empirical equation and the crystal field consideration coincide with temperature dependence of the emission bands.

Supporting Information

Further details of the crystal structure may be obtained from the Fachinformationszentrum Karlsruhe, D-76344 Eggenstein-Leopoldshafen, Germany (fax: (49) 7247-808-666; e-mail: crysdata@fiz-karlsruhe.de) on quoting the depository number CSD-422406 for $BaCa_2MgSi_2O_8$.

Acknowledgment

The authors would like to thank Dr. Y.N. Choi in the Korea Atomic Energy Institute, Daejeon, Korea, for assistance with the neutron powder diffraction measurement.

Appendix A. Supplementary material

Supplementary data associated with this article can be found in the online version at doi:10.1016/j.jssc.2011.04.030.

References

[1] T. Kano, in: S. Shionoya, W.M. Yen (Eds.), Phosphor Handbook, CRC Press, Boca Raton, 2000, p. 192.
[2] G. Blasse, W.L. Wanmaker, J.W. Vrugt, A. Bril, Philips Res. Rep. 23 (1968) 189–200.
[3] T.L. Barry, J. Electrochem. Soc. 115 (1968) 733–738.
[4] J.S. Kim, P.E. Jeon, J.C. Choi, H.L. Park, S.I. Mho, G.C. Kim, Appl. Phys. Lett. 84 (2004) 2931–2933.
[5] H.K. Jung, K.S. Seo, Opt. Mater. 28 (2006) 602–605.
[6] J.S. Kim, A.K. Kwon, Y.H. Park, J.C. Choi, H.L. Park, G.C. Kim, J. Lumin. 122-123 (2007) 583–586.
[7] Y. Lin, Z. Zhang, Z. Tang, X. Wang, J. Zhang, Z. Zheng, J. Eur. Ceram. Soc. 21 (2001) 683–685.
[8] Y. Yonesaki, T. Takei, N. Kumada, N. Kinomura, J. Lumin. 128 (2008) 1507–1514.
[9] Y. Yonesaki, T. Takei, N. Kumada, N. Kinomura, J. Solid State Chem. 182 (2009) 547–554.
[10] H.A. Klasens, A.H. Hoekstra, A.P.M. Cox, J. Electrochem. Soc. 104 (2) (1957) 93–100.
[11] P.B. Moore, T. Araki, Am. Miner. 57 (1972) 1355–1374.
[12] T. Aitasalo, A. Hietikko, J. Hölsä, M. Lastusaari, J. Niittykoski, T. Piispanen, Z. Kristallogr. Suppl. 26 (2007) 461–466.
[13] C.H. Park, S.T. Hong, D.A. Keszler, J. Solid State Chem. 182 (2009) 496–501.
[14] R.D. Shannon, C.T. Prewitt, Acta Crystallogr B35 (1969) 925–946.
[15] R.W. Cheary, A. Coelho, J. Appl. Crystallogr. 25 (1992) 109–121; Bruker AXS, TOPAS 3, Karlsruhe, Germany (2000).
[16] I.D. Brown, D. Altermatt, Acta Crystallogr. B 41 (1985) 244–247.
[17] N.E. Brese, M. O'Keeffe, Acta Crystallogr. B 47 (1991) 192–197.
[18] I.D. Brown, Chem. Rev. 109 (2009) 6858–6919.
[19] L.G. Van Uitert, J. Lumin. 29 (1984) 1–9.
[20] C.-H. Park, Y.-N. Choi, J. Solid State Chem. 182 (2009) 1884–1888.
[21] G. Blasse, J. Chem. Phys. 51 (1969) 3529–3530.
[22] B. Henderson, G.F. Imbusch (Eds.), Optical Spectroscopy of Inorganic Solids, Clarendon Press, Oxford, 1989.
[23] G. Blasse, A. Bril, Philips Tech. Rev. 31 (1970) 304–332.
[24] G. Blasse, W.L. Wanmaker, J.W. ter Vrugt, J. Electrochem. Soc. 115 (1968) 673–677.